

PHYSICS OF A HIGH-LUMINOSITY TAU-CHARM FACTORY‡

MARY E. KING

*Stanford Linear Accelerator Center,
Stanford University, Stanford, CA 94309, U.S.A.*

ABSTRACT

This paper highlights the physics capabilities of a Tau-Charm Factory; i.e., a high luminosity ($\sim 10^{33} \text{cm}^{-2} \text{s}^{-1}$) e^+e^- collider operating in the center-of-mass energy range of 3-5 GeV, with a high-precision, general-purpose detector. Recent developments in τ and charm physics are emphasized.

*Invited talk presented at Second Workshop on Tau Lepton Physics,
The Ohio State University, Columbus, Ohio, USA, September 8-11, 1992*

‡Work supported by the U.S. Department of Energy under Contract DE-AC03-76SF00515.

1. Introduction

The Tau-Charm Factory (TCF) is conceived as a high luminosity ($\sim 10^{33} \text{ cm}^{-2}\text{s}^{-1}$) e^+e^- collider operating in the center-of-mass energy range of 3-5 GeV, with a high-precision, general-purpose detector. The TCF physics program is broad, encompassing τ and charm production and decay studies near threshold, and studies of bound-state charmonium production and decay. The ability to run at, above, or below particle production threshold gives unique kinematic constraints and control of systematic errors. At design luminosity, the collider will produce 10^8 τ pairs/yr, 10^8 charmed mesons/yr, and 10^{10} - 10^{11} J/ψ /yr, far exceeding the production rate for these particles at present facilities. The TCF general-purpose detector is designed to be fully hermetic, and of uniformly high precision for all particle types. The combination of high statistics with a high precision detector and the ability to vary center-of-mass energy around production threshold makes the TCF unique. Additionally, it is the only future high luminosity machine dedicated to τ and charm physics.

2. TCF Machine

The TCF machine is designed to achieve a luminosity of about $10^{33} \text{ cm}^{-2}\text{s}^{-1}$. The luminosity lifetime, limited predominantly by beam-beam bremsstrahlung, is about two hours. The TCF machine features double rings with electrostatic separators to minimize parasitic crossings of the beams in the IP region.¹ Each ring has a 360 m circumference and contains about 30 bunches, with a collision frequency of 25 MHz. The IR design involves superconducting final focus quadrupole triplets that penetrate ± 80 cm from the IP into the detector volume, and vertical separators that start 3.5 m from the IP. The machine design incorporates monochromator optics, so that cms energy spreads near 100 keV can be achieved. Energy monochromatization facilitates production of the J/ψ at a rate of 2×10^{11} /yr for CP studies in the hyperon system, and increased production at the τ threshold. Beam polarization may also be available for energy calibration and for improving the sensitivity of the CP studies.

3. Particle Production Rates

A luminosity $\sim 10^{33} \text{ cm}^{-2}\text{s}^{-1}$ coupled with a dedicated injector (assume 2×10^7 s/yr running time) gives the TCF the ability to produce large numbers of τ and charmed

particles, giving adequate statistics to search for the first time for rare processes at the 10^{-7} - 10^{-8} level. Figure 1 shows the τ cross section and hadronic rate as a function of center-of-mass energy. Running at the peak τ cross section of 4.25 GeV, 1.6×10^8 τ particles/yr can be produced. Running below the ψ' threshold at 3.67 GeV, 5.5×10^7 τ particles/yr can be created, and running at threshold (without using monochromator optics), 1.1×10^7 τ particles/yr are made. For comparison, a future CLEO II upgrade could produce $\sim 10^7$ τ pairs, and CLEO II presently has the largest τ sample, containing $\sim 1.3 \times 10^6$ τ pairs. CESR and ARGUS each produced about 10^5 τ pair events, while SPEAR produced on the order of 10^4 .

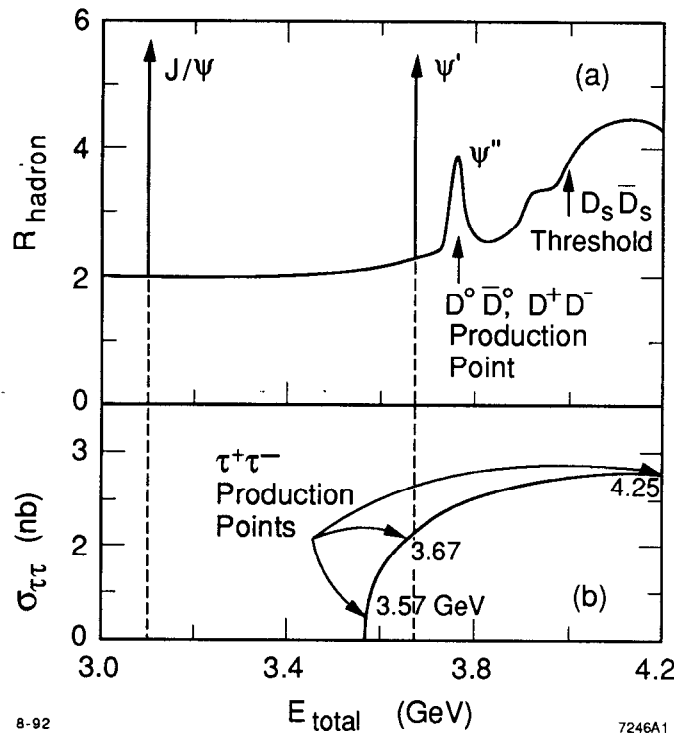


Figure 1. Hadronic Rate and τ Cross Section as function of center-of-mass energy.

A significantly larger data sample of charmed mesons can also be produced and tagged at the TCF than at existing experiments. At the TCF, it is possible to produce (tag) 0.8×10^8 (5.6×10^6) $D^+ D^-$ /yr and 1.2×10^8 (1.4×10^7) $D^0 \bar{D}^0$ /yr, at $E_{cm} = 3.77$, or 4×10^7 (1.3×10^6) $D_s D_s^*$ /yr at $E_{cm} = 4.14$ GeV. Fixed target experiments come closest to approaching these statistics: E791 will tag a few times 10^5 D events, while E691 tagged about 10^4 D events. With the MARK III, ~ 5000 D events were identified.

4. TCF Detector

To fully exploit the machine's high luminosity for physics studies, the detector design and performance is critical.² The TCF detector (Figure 2) features a long barrel ($|\cos\theta| < 0.95$) containing a low-Z gas drift chamber, followed by a 4 m long, two-layer scintillating fiber TOF system. Unlike the B-Factory, at the TCF, TOF for particle ID is adequate, and the TOF scintillator does not compromise the performance of the calorimeter immediately behind it. The calorimeter consists of longitudinally-segmented CsI(Tl) or CsI(Na) crystals, with $\sim 8,000$ - $10,000$ crystal towers arranged in projective geometry. The long barrel design avoids a significant endcap region, and the detector is closed by a forward silicon tracking system and BaF₂ calorimeter. The 8 kG magnet is followed by a fine-grained muon system that acts as a flux return. It also serves as a veto for neutral hadron energy, such that neutrinos can be tagged by missing energy.

All aspects of the detector design have been influenced by physics analysis considerations. For example, the tracking-system momentum-resolution design goal, $\delta p / p = 0.3\% + 0.3\%p$, is motivated by the desire to accurately measure the endpoint in the invariant mass spectrum of the decay $\tau \rightarrow 5\pi + \nu_\tau$. Similarly, the 120 ps time resolution of TOF system design is based on achieving $>3\sigma$ background rejection in the measurement of $D^0\bar{D}^0$ mixing. A CsI calorimeter facilitates measuring photons and charged tracks to a similar precision, and makes possible the utilization of photons down to 10 MeV in energy. These capabilities are particularly useful in untangling branching ratios and in the detection of rare processes. The capability of the muon system to act as a veto for neutral hadron energy is an important factor in the study of rare decays, and in the tagging of τ events.

5. Highlights of Tau Physics at a Tau-Charm Factory

The TCF has the capability to make numerous benchmark measurements involving the τ lepton and τ neutrino, including measurements of the τ and ν_τ mass, precision τ branching ratio measurements, searches for rare and forbidden τ decays, studies of the Lorentz structure of the $\tau - \nu_\tau - W$ vertex, W^\pm hadronization, and CP violation in the lepton sector. The TCF capabilities for making these measurements have been reviewed extensively elsewhere.³ Selected recent measurements in τ physics, and the capability of the TCF to address the issues they raise, will be discussed here.

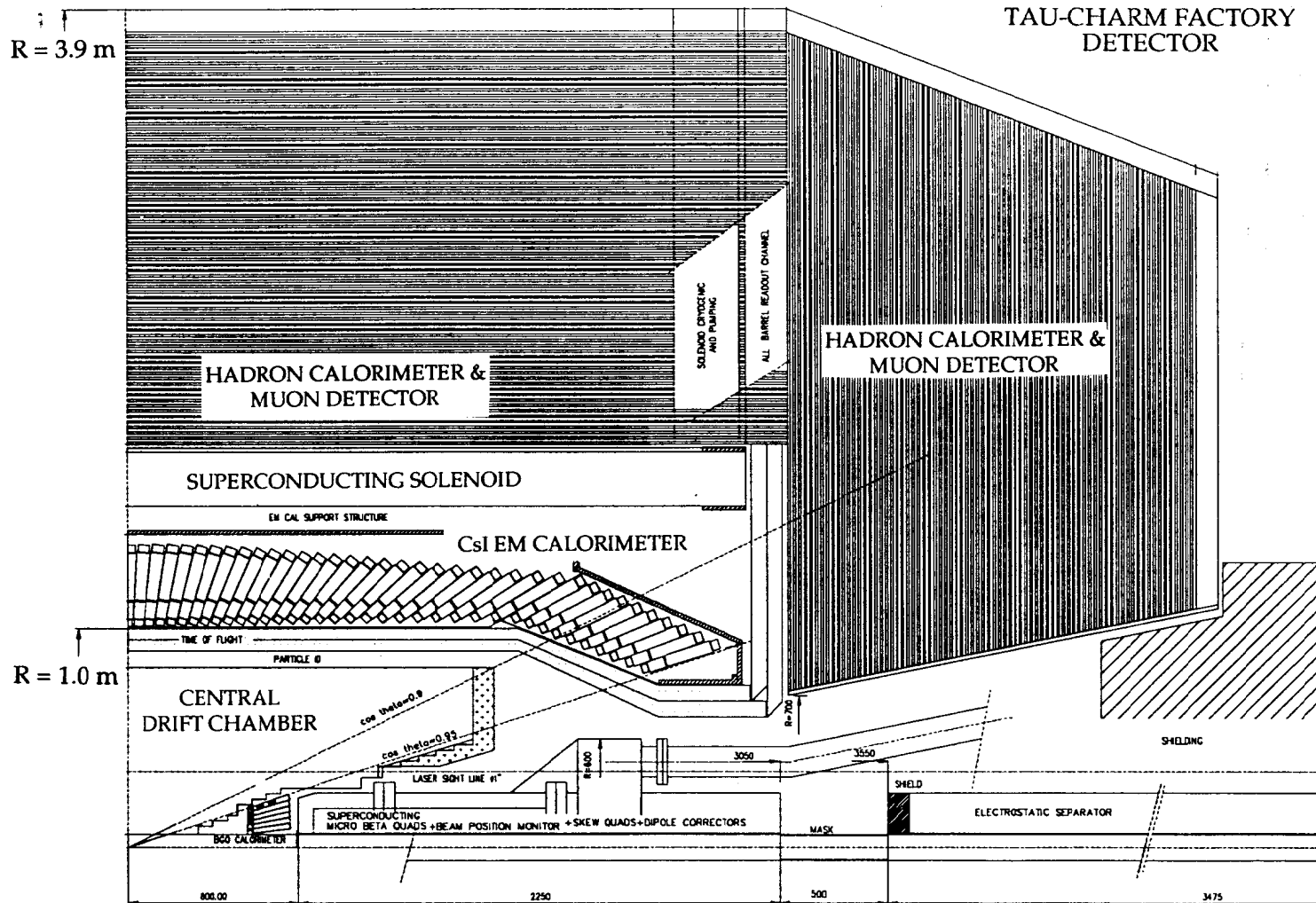


Figure 2. Side view of TCF detector showing detector subsystems, including low-Z gas drift chamber, time-of-flight scintillator, CsI crystal system, magnet, hadron calorimeter, and forward calorimeter and silicon tracking system.

5.1 *Tau Neutrino Mass Measurement*

The Standard Model does not predict the masses of any of the fundamental fermions. Measurements from SLC and LEP, as well as from astronomy,⁴ indicate that there are no fourth generation neutral leptons with mass $< 45 \text{ GeV}/c^2$. The issue remains as to whether or not the three known neutrino types have mass. If the neutrinos do have mass, mixing and oscillations between lepton families could occur, and nonzero neutrino mass could provide answers to the solar neutrino deficiency and the composition of dark matter.⁵ The current mass limits are $m(\nu_e) < 13 \text{ eV}$,⁶ $m(\nu_\mu) < 270 \text{ keV}$,⁷ and $m(\nu_\tau) < 31 \text{ MeV}$.⁸

Some models allow strict limits to be placed on ν_e and ν_μ masses based on a ν_τ mass limit. For example, in the see-saw model, $m(\nu_i)$ is proportional to $m(l)^2$, so a sensitivity of $1 \text{ MeV}/c^2$ for $m(\nu_\tau)$ gives a limit of $0.1 \text{ eV}/c^2$ for $m(\nu_e)$.⁷ For this reason, a significantly better limit on the ν_τ mass is extremely desirable; however, the most recent ν_τ mass measurement, by CLEO II, resulted in a limit of $m(\nu_\tau) < 34.4 \text{ MeV}$ @ 95% CL,¹¹ a mass limit greater than the new limit set by ARGUS, but with significantly higher statistics. The ν_τ mass was measured by CLEO and ARGUS using the invariant mass spectrum in the decay $\tau \rightarrow 5\pi + \nu_\tau$. Depending on the ν_τ mass, the shape of the endpoint spectrum is different. In the ARGUS and CLEO II measurements, the limiting factors to achieving a better mass limit are statistics, background rejection, and resolution at the endpoint.

The TCF design is such that the ν_τ mass limit can be improved by an order of magnitude over existing limits.¹² The TCF detector's central drift chamber momentum resolution is driven by the goal of excellent resolution of the endpoint of the invariant mass spectrum of the $\tau \rightarrow 5\pi + \nu_\tau$ decay. (Refer to Section 4.) The high luminosity of the TCF machine gives a much larger data sample, and the ability to run near threshold greatly reduces backgrounds from non- τ events. For example, running at $E_{cm} = 3.68 \text{ GeV}$ results in high τ -pair production rates without producing charmed mesons, a potentially dangerous background. With a 20 fb^{-1} data sample running at 3.67 GeV , 350 signal and 0 background events pass selection criteria. Figure 3 shows the endpoint of the $5\pi\nu_\tau$ invariant mass spectrum for various ν_τ masses, as seen in the TCF detector using

computer simulations. If $m(\nu_\tau) = 0$, a limit of $3.5 \text{ MeV}/c^2$ can be set at the 95% CL, in one year.

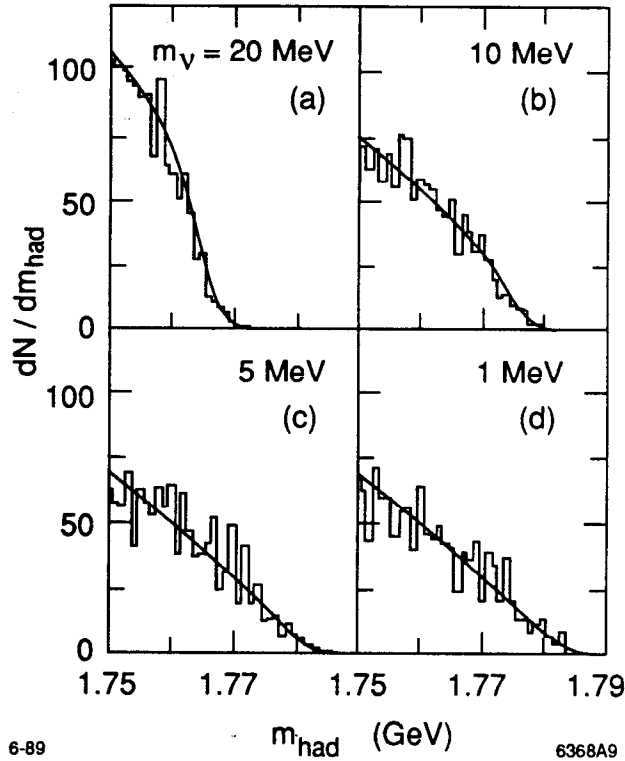


Figure 3. Endpoint of $\tau \rightarrow 5\pi + \nu_\tau$ invariant mass spectrum from τ decays, for various $m(\nu_\tau)$.

For $m(\nu_\tau) \geq 100 \text{ eV}$, an indirect method can also be utilized to set a ν_τ mass limit.¹³ Cosmological arguments indicate that any neutrino with mass greater than $\sim 100 \text{ eV}/c^2$ must be unstable. The tau neutrino could decay through the process $\nu_\tau \rightarrow l + X$ ($l = e, \mu$), where X is a massless, weakly interacting Goldstone boson (Majoron, familon, flavon, etc.). The τ would decay through the same process; i.e., $\tau \rightarrow l + X$ ($l = e, \mu$), and the branching ratios are in the range of 10^{-6} to 10^{-2} . The present limits for these decay modes are 1-2%. At the TCF, 2σ limits can be set that are two-to-three orders of magnitude better than the existing limits. The search technique involves looking for a peak in the normalized spectrum of electron energy in τ decays to an electron. The peak could represent the decay $\tau \rightarrow e + X$ folded in with the standard decay $\tau \rightarrow e \nu_e \nu_\tau$. The peak is visible running near the τ threshold, but is smeared out at high energies because tracks in the event are boosted.

Combining these two techniques, the TCF has the capability to set a ν_τ mass limit down to $100 \text{ eV}/c^2$, with implications from theory for the masses of the two other neutrino types.

5.2 *Tau Branching Ratios*

At the TCF, it will be possible to reduce the fractional error on τ one-prong branching ratios by an order of magnitude or more over existing measurements. There are many motivations for making precision measurements of these branching ratios. For example, the Standard Model makes many predictions about τ decay rates and angular and helicity distributions, and these predictions can be used to look for interactions beyond those predicted by the Standard Model. In this context, also of interest is the potential discrepancy between the inclusive $\tau \rightarrow$ one-prong branching ratio and the sum of the exclusive one-prong decays.

Measurements of the τ leptonic branching ratios and the τ lifetime also provide a test of lepton universality. The most precise measurement of $B(\tau \rightarrow e\nu_e\nu_\tau)$ to date has been made by CLEO II, giving $B_e = 17.49 \pm 0.14 \pm 0.22\%$.¹⁴ Using summary data presented at DPF92,¹⁴ the combined τ lifetime from the LEP experiments is $292 \pm 3 \pm 2$ fs. These quantities are shown in Figure 4, where the statistical and systematic errors are shown separately. (The systematic errors may be interpreted as the full range in which the quoted measurements are valid, rather than as Gaussian errors.) Also shown is the range of values predicted by the Standard Model for $B(\tau \rightarrow e\nu_e\nu_\tau)$ and τ lifetime, where the new τ mass measurement from BES, $m(\tau) = 1776.9 \pm 0.3 \pm 0.2$,¹⁴ has been utilized. It is not clear that the measured values are entirely in accord with lepton universality. However, a measurement of $B(\tau \rightarrow e\nu_e\nu_\tau)$ at the TCF, with fractional errors at the 0.1% level, could clarify this issue.

Branching measurements to this level of precision can be made at the TCF utilizing its unique features. The ability to run near threshold means that the π and K momentum spectra are well-separated from e and μ momentum spectra of single-charged particles in τ decays, as shown in Figure 5. This gives the possibility of several unique signatures with which to single-tag τ events, such as $e + E_{\text{miss}}$, $\mu + E_{\text{miss}}$, and monochromatic $\pi + E_{\text{miss}}$, as well as good π/K separation capabilities. Precise missing energy measurements are made feasible with the hermetic detector, including the

electromagnetic calorimeter which can measure photons down to 10 MeV in energy, and the fine-grained hadron calorimeter, which detects K_L^0 's and n 's. Given the monochromatic nature of the π and K decays, particle identification only requires discriminating between $K-\mu-e$ and $\pi-\mu-e$, such that a misidentification rate of $< 10^{-3}$ can be achieved.¹⁵ In contrast, at higher energies the one-prong momentum spectra from τ decays completely overlap, making particle identifications requirements more severe.

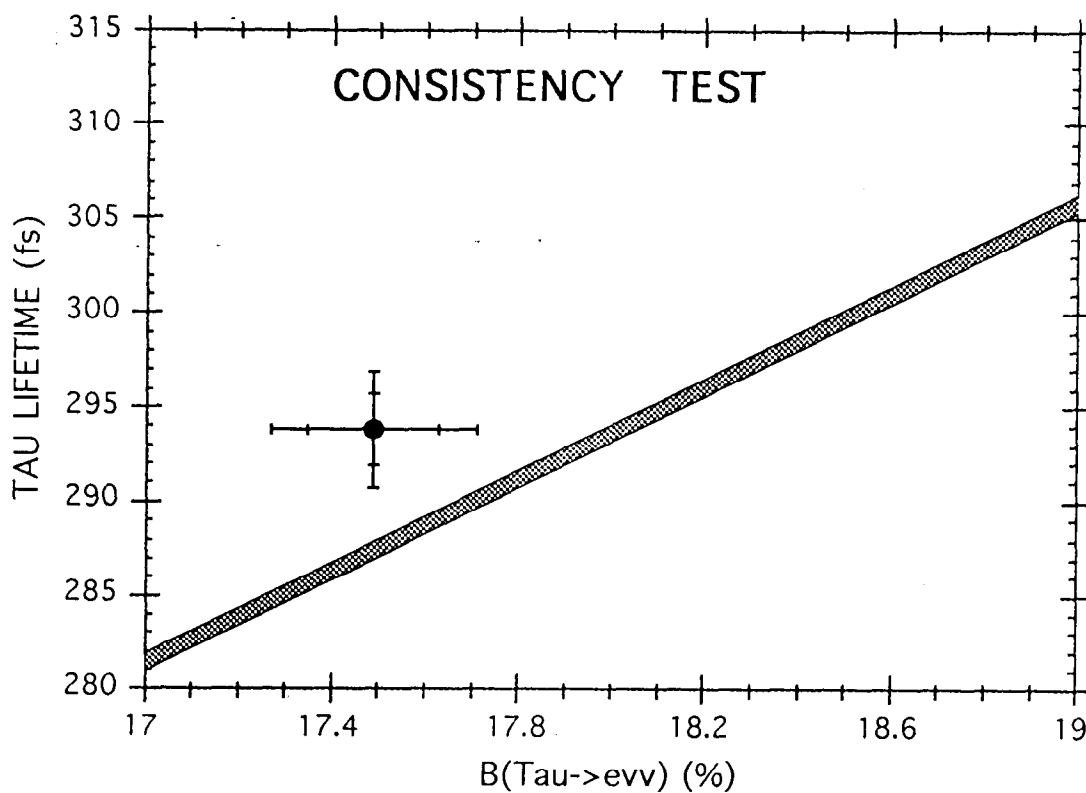


Figure 4. Lepton Universality as indicated by theory (shaded region) and by experiment (data point, where statistical and systematic errors are shown separately). Data is current CLEO $B(\tau \rightarrow e\nu_e\nu_\tau)$ measurement and current LEP average lifetime measurement (see text).

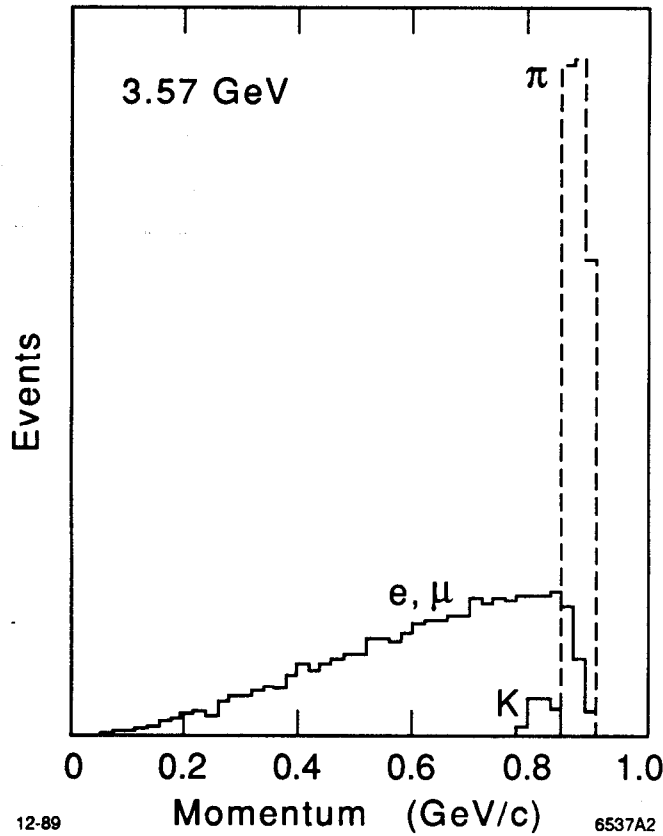


Figure 5. Momentum spectra of one-prong particles in τ decays.

6. Highlights of Charm Physics at a Tau-Charm Factory

In addition to many significant contributions to τ physics, the TCF also has the capability to make many seminal studies in charm physics. The most unique contributions of the TCF in charmed meson studies will be: (1) measurement of the pure leptonic decays of D^+ and D_s , yielding f_D and f_{D_s} , (2) studies of second order weak interactions ($D^0\bar{D}^0$ mixing) and setting of limits on CP violation in charm meson decays, (3) measurement of the semileptonic decays of D^+ and D_s , giving KM matrix parameters and the lepton spectrum, and (4) searches for rare D^0 , D^+ , and D_s decays, measurement of radiative and hadronic penguin events, and searches for decays outside of the Standard Model.¹⁶ Note that the charm physics program greatly compliments any program that studies B -meson decays at a similar precision. Only one of these topics, the measurement of the pure leptonic decays, will be discussed here.

6.1 Leptonic Decays of D Mesons

The pure leptonic decays of D^+ and D_s are presently unexplored; however, they allow determination of f_D and f_{D_s} , and give the potential for extrapolating f_B .¹⁷ The decay constants f_D and f_{D_s} characterize the degree of overlap of c and d quarks in the D^+ , and c and s quarks in D_s , respectively, so they contain all QCD corrections which modify the $Wq\bar{q}$ vertex from a pure weak interaction. They also appear in calculations of annihilation and exchange processes. In particular, they are relevant for second order weak interactions, such as heavy meson mixing.

The constants can be determined by precision measurements of the leptonic branching ratios $B(D^+ \rightarrow \mu^+ \nu)$ and $B(D_s \rightarrow \mu^+ \nu_\mu)$. The former is given by:

$$B(D^+ \rightarrow \mu^+ \nu) = \frac{G_F^2}{8\pi} f_D^2 \tau_D M_D m_\mu^2 |V_{cd}|^2 \left(1 - \frac{m_\mu^2}{M_D^2}\right)^2, \quad (1)$$

where M_D is the meson mass, m_μ the muon mass, V_{cd} the KM matrix element, and τ_D the D^+ lifetime, and the formula for the latter is obtained by substituting $M_D \rightarrow M_{D_s}$, and $V_{cd} \rightarrow V_{cs}$. In simple nonrelativistic models, decay constants such as f_D and f_{D_s} scale like the square root of the inverse of the heavy quark mass (the $1/M_D$ term) times the reduced mass of the heavy and light quark to a power between one and two (the $\psi(0)$ term). The $1/M_D$ dependence appears to be reproduced in lattice calculations.¹⁷ Consequently, by measuring f_D and f_{D_s} to adequate precision, it should be possible to distinguish among models predicting their values. Then it would be possible to extrapolate to the heavier B system, for which experimental measurements may never be obtainable, to extract a value for f_B .

As alluded to above, the importance of the weak decay constants goes beyond the pure leptonic processes, and extends to all second-order weak processes involving hadrons. Of particular interest is $D\bar{D}$ and $B\bar{B}$ mixing involving box diagrams, the evaluation of which requires understanding of the QCD corrections embodied in the decay constants. For example, in the equation describing $B\bar{B}$ mixing, the largest unknowns are the B_d lifetime, f_{B_d} , and the B_{B_d} parameter. Since B_{B_d} describes QCD corrections for internal gluon lines to the box diagram, its calculation is directly related to the calculation of f_B .

At the TCF, the measurement of $D^+ \rightarrow \mu^+ \nu_\mu$ and $D_s \rightarrow \mu^+ \nu_\mu$ are straightforward. D events are single-tagged, and events are sought containing only one additional particle, a muon, and with missing mass near zero. In the D rest frame, the muon is monochromatic. After kinematic cuts from tagging, the major backgrounds that remain are from two-body hadronic channels and from semi-muonic decays. By vetoing a K_L^0 's and using detector hermeticity for photons, these backgrounds can be reduced to less than a few percent. Using these techniques at TCF, f_D and f_{D_s} can be measured to a few percent.

7. Highlights of Charmonium and Light Quark Spectroscopy at TCF

In addition to extensive programs for the study of τ and charm physics, a strong parallel program of charmonium, light quark, and gluonium spectroscopy is accessible at TCF, with little impact on the τ and charm physics programs. It includes studies of charmonium systems (η_c, χ), search for gluon-gluon bound states, and the possibility of direct CP violation measurements in hyperon ($\Xi\bar{\Xi}, \Lambda\bar{\Lambda}$) decays.

8. Conclusion

The TCF design uniquely incorporates a high luminosity machine, capable of running at various energies around particle production thresholds, with a high-precision (uniform for all particles), fully hermetic detector. This powerful combination gives the capability to make many significant, precision measurements in τ , charm, and charmonium physics, illuminating these systems and possibility leading beyond the Standard Model.

Acknowledgments

I would like to thank the many physicists in the United States and abroad who have worked to develop the TCF and understand its physics potential. I am particularly grateful to Professors Martin Perl and Rafe Schindler for many stimulating discussions about TCF issues.

References

1. J. M. Jowett, in *1989 Proceedings of Tau-Charm Factory Workshop*, ed. L. Beers, SLAC-REPORT-343 (SLAC, Stanford), 7.
2. R. H. Schindler, "Status of the Tau-Charm Factory Project and Aspects of Detector Design," talk presented at the 26th International Conference in High Energy Physics, Dallas, TX, August 6-12, 1992.
3. See, for example:
Proceedings of the Tau-Charm Factory Workshop, edited by L. Beers, SLAC-REPORT-343 (SLAC, Stanford).
M. Perl & R. H. Schindler, "The Tau-Charm Factory: Experimental Perspectives," talk presented at the Tau-Charm Factory Workshop, Universidad de Sevilla, Andalucia, Spain, April 29-May 2, 1991, and published as SLAC-PUB-5666.
J. Kirkby, in *Workshop on Tau Lepton Physics*, edited by M. Davier and B. Jean-Marie (Editions Frontieres, Gif-sur-Yvette Cedex, 1991), p. 453.
4. *Phys. Rev. D* **45**, 1992, VI.30.
5. H. Harari & Y. Nir, *Nucl. Phys. B* **292**, 1987, 251.
6. H. Kawakami *et al.*, *Phys. Lett. B* **256**, 1991, 105.
7. R. Abela *et al.*, *Phys. Lett. B* **146**, 1984, 431.
8. Result presented by D. Britton at Second Workshop on Tau Lepton Physics, The Ohio State University, Columbus, Ohio, USA, September 8-11, 1992.
9. Result presented by D. Cowan at Second Workshop on Tau Lepton Physics, The Ohio State University, Columbus, Ohio, USA, September 8-11, 1992.
10. J. J. Gomez-Cadenas *et al.*, *Phys. Rev. D* **41**, 1990, 2179-2186.
11. J. W. F. Valle, in talk presented at Second Workshop on Tau Lepton Physics, The Ohio State University, Columbus, Ohio, USA, September 8-11, 1992.
R. Alemany, J.J. Gomez-Cadenas, M.C. Gonzalez-Garcia and J.W.F. Valle, "Exotic Tau Decays", CERN Preprint, FTUV/92-58, IFIC/92-56.
12. Results presented at 7th Meeting of the American Physical Society Division of Particles and Fields, November 10-14, 1992, as summarized by W. Toki in Tau Decays talk.
13. J. Kirkby, in *Workshop on Tau Lepton Physics*, edited by M. Davier and B. Jean-Marie (Editions Frontieres, Gif-sur-Yvette Cedex, 1991), p. 453.

14. R. H. Schindler, in *Proceedings of the Fifth Lake Louise Winter Institute, The Standard Model and Beyond*, Chateau Lake Louise, 1990, edited by A. Astbury *et al.*, (World Scientific, Singapore, 1990).
15. R. H. Schindler, in *Les Recontres de Physique de la Vallee D'Aoste: Results and Perspectives in Particle Physics*, edited by M. Greco. (Editions Frontieres, Gif-sur-Yvette-Cedex, 1989).
16. A. Soni, private communication to R. H. Schindler, and C. Bernard *et al.*, *Phys. Rev. D* **38**, 1988, 3540.